"This document is the unedited Author's version of a Submitted Work that was subsequently accepted for publication in Nano Letters, copyright © American Chemical Society after peer review. To access the final edited and published work see http://pubs.acs.org/doi/abs/10.1021/nl802295n."

NANO LETTERS
2008
Vol. 8, No. 11
3865-3869

Sub-10 nm Nanoimprint Lithography by Wafer Bowing

Wei Wu,*,† William M. Tong,†,‡ Jonathan Bartman,‡ Yufeng Chen,‡ Robert Walmsley,† Zhaoning Yu,† Qiangfei Xia,† Inkyu Park,† Carl Picciotto,† Jun Gao,† Shih-Yuan Wang,† Deborah Morecroft,§ Joel Yang,§ Karl K. Berggren,§ and R. Stanley Williams†

HP Laboratories, Hewlett-Packard Co., Palo Alto, California 94304, Hewlett-Packard Co., Corvallis, Oregon 97330, and Massachusetts Institute of Technology, Cambridge, Massachusetts 02139

Received July 29, 2008; Revised Manuscript Received September 11, 2008

ABSTRACT

We introduce the concept of wafer bowing to affect nanoimprinting. This approach allows a design that can fit the key imprinting mechanism into a compact module, which we have constructed and demonstrated with an overlay and resolution of <0.5 μm and <10 nm, respectively. In the short term, this wafer bowing approach makes nanoimprint lithography much more accessible to a broad range of researchers. More importantly, this approach eliminates machine movement other than wafer bowing and shortens the mechanical path; these will enable the achievement of excellent patterning and overlay at a much lower cost. In the long term, wafer bowing is extensible to step-and-repeat printing for volume manufacturing.

Nanoimprint lithography (NIL)[1] is a low cost nanopatterning technology based on the mechanical deformation of a resist. It challenges traditional photolithography in high-resolution patterning. We have employed NIL to fabricate crossbar structures with half-pitch down to 17 nm,[2] isolated nanowires with 6 nm line width, and other functional applications for nanoelectronics[3] and nanophotonics.[4,5] While the resolution of nanoimprint has exceeded that of photolithography, it is still in the nascent phases of development. Fundamentally, nanoimprint is a mechanical contact rather than optical process, and therefore has a different set of challenges: how to preserve alignment and the subsequent overlay during mold approach, how to apply contact force uniformly, and how to prevent air from being trapped between the mask and the substrate. Conventional approaches to meet those challenges have been to improve the mechanical stability of the system and to use ultraflat templates and double-sided polished wafers; these inevitably add cost that can potentially take away the value advantage of nanoimprint lithography.

With a focus on achieving good results but at a low cost, we devised a novel wafer-bowing scheme to affect approach and imprint. In our scheme, the imprint force is applied uniformly and systematically from center to edge, preventing air from being trapped. More importantly, it shortens the mechanical path between the mold and wafer; this makes the imprinter less susceptible to ambient vibration and helps to preserve the alignment during mold-wafer approach. After an UV exposure step, air can be let into the module to effect mold-wafer detachment. All this is carried out without sophisticated machinary, keeping the cost low. The compact design allows the entire module to be fitted into a commercial contact mask aligner in place of the wafer chuck and transform it into a nanoimprint machine with the inherent alignment capability of the contact aligner. Moreover, our concept is extensible to a step-and-repeat scheme required for volume manufacturing.

Principle of Operation. Our mold or template is a 5 in. photomask. The key enablers of our concept were spacers with precise heights deposited around the imprint areas. These spacers, which are located outside the perimeter of the imprint field (i.e., the streets), spatially offset the wafer from the mask while maintaining the two surfaces within a short distance and close parallelism during the fine alignment phase. These are critical both for keeping the mask and wafer alignment marks simultaneously in focus and for maintaining the alignment during approach and contact. Indeed the precise control of the spacer heights is critical, but this is not a challenge as today's deposition and etching processes easily give features with better than one nanometer thickness uniformity.

The nanoimprint process is divided into the following steps: (1) coarse alignment, (2) fine alignment, (3) approach and imprint, and (4) release (Figure 1). Coarse alignment is

* To whom correspondence should be addressed. E-mail: wei.wu@hp.com.
† HP Laboratories, Hewlett-Packard Co., Palo Alto, CA.
‡ Hewlett-Packard Co., Corvallis, OR.
§ Massachusetts Institute of Technology.

10.1021/nl802295n CCC: $40.75 © 2008 American Chemical Society
Published on Web 10/07/2008

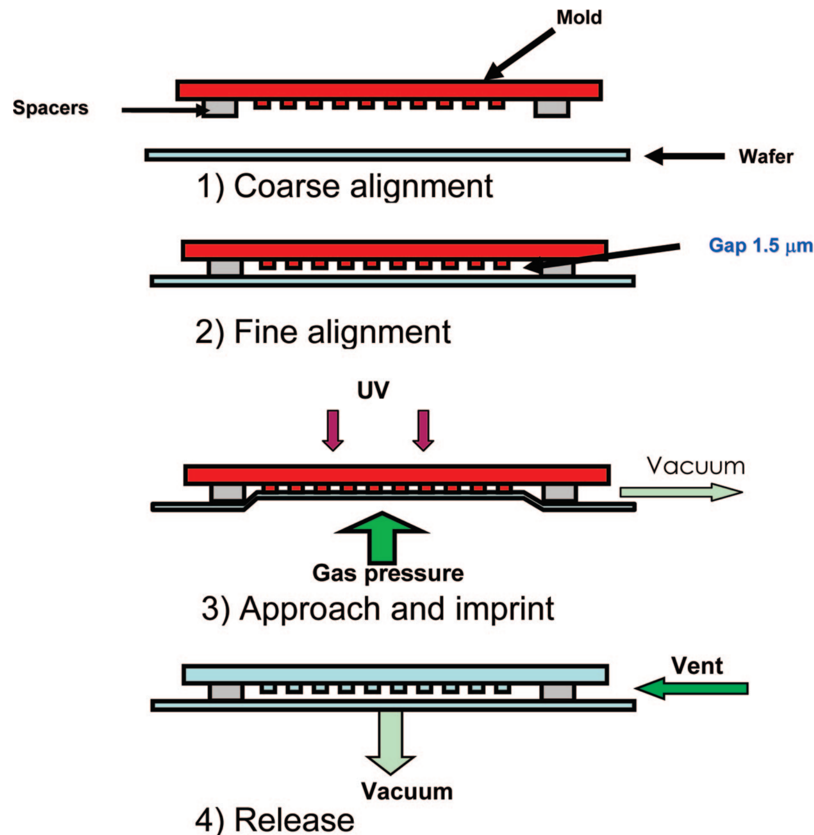

Figure 1. Schematic diagram of the nanoimprint module work flow.

performed without the mask and substrate in contact with an accuracy of 1 μm, after which the mask (more specifically the spacers on the mask) are brought into contact with the substrate. During fine alignment the spacers slide on the streets of the substrate to keep the mask and substrate exactly parallel with a gap the same as the spacer height. It is important to point out that the sliding occurs only during the fine alignment and its magnitude is <1 μm; the spacers are designed to be located in the street area on the substrate, so that no patterns will be destroyed during spacer sliding. In approach and imprint, the air between the wafer and the mask is pumped out and gas pressure can be applied to the backside of the wafer (or the mask). The wafer and the mask are pressed onto each other because one or both bow under the applied pressure, transferring the patterns into the resist. The nanoimprint resist is then cured by exposure to UV light. To facilitate the release of the mask from the wafer, air is vented into the gap between the wafer and the mask and a vacuum is applied to the backside of the wafer, after which the imprint process is completed.

Our approach has the following advantages: (1) there is no local mechanical movement other than wafer bowing during the approach and imprint, thus preserving the alignment during the process; (2) the mask and the substrate are in contact through the spacers during the fine alignment step, so that the mechanical path between the nanoimprint mask and substrate is minimized for better mechanical stability; (3) our wafer-bowing method ensures that the imprint pressure is uniform and without lateral components in the imprint field; (4) during the imprint process, the center of the imprint area reaches contact first and then spreads out to the edges, preventing air from being trapped between the mask and substrate; and (5) the mold and wafer separation is facilitated simply by releasing the gas pressure.

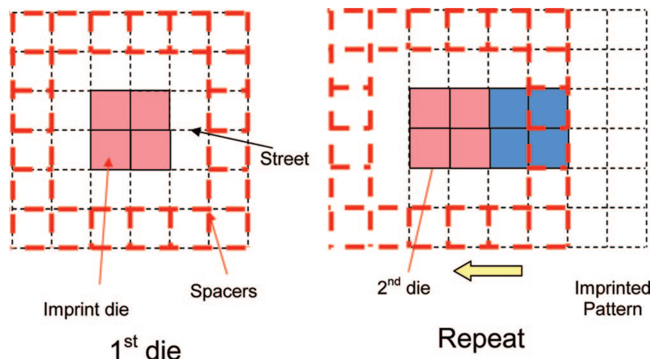

Figure 2. Schematic diagram of a step-and-repeat process. The spacers only make contact with the wafers in the streets area. The wafer is divided into an array of zones and those zones can be vacuumed and vented individually to realize wafer bowing at each die.

The focus of this paper is to illustrate our wafer-bowing method by demonstrating a low-cost module that can be placed in a mask aligner to achieve imprint with the inherent overlay capability of the mask aligner. The advantages of this method allow us to construct a system with the overlay performance of a conventional nanoimprinter but at a much lower cost. Figure 2 illustrates that our wafer-bowing method can be extended to step-and-repeat volume manufacturing.

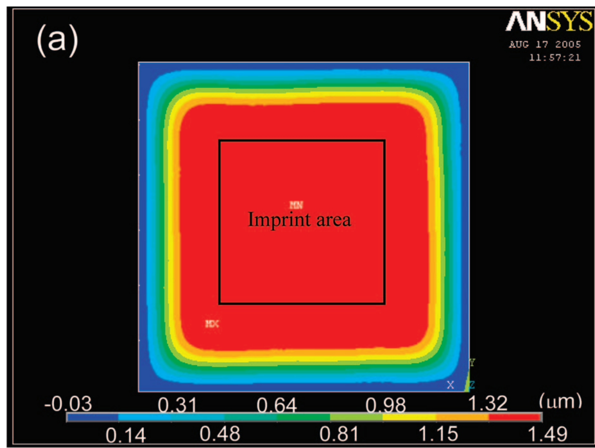

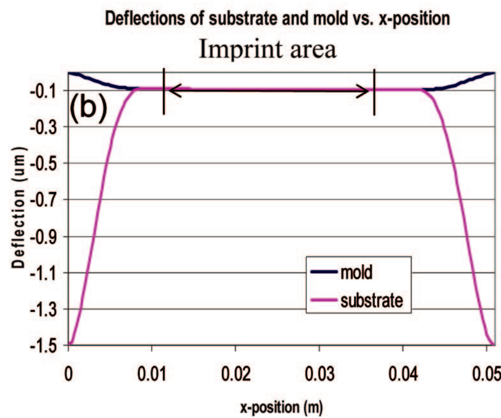

Figure 3. Numerical simulation (FEM) results of the wafer bowing in the "*z*" direction. (a) The 2D map of the wafer displacement in the "*z*" direction. (b) The profile of the wafer displacement in the "*z*" (pink line) and mask displacement in "*z*" (blue line). They show a uniform contact formed over the whole imprint filed.

Modeling of the Wafer Bowing. The key distinguishing difference of our nanoimprint technology is that it affects the approach and imprint with wafer (or/and mask) bowing. There had been concerns that the bowing can result in lateral shift of the patterns and lead to registration error. We modeled this process with a finite element method (FEM) numerical simulation to demonstrate that wafer and mask bowing can achieve uniform imprint contact within the entire imprint area (Figure 3). In the simulated configuration, the field size is 25.4 mm × 25.4 mm (1 in. × 1 in.), the distance between the nearby spacers to the nanoimprint field was 12.7 mm, the spacer height was 1.5 μm, and the substrate was a standard 4 in. Si wafer. Figure 3 shows that most of the distortion is localized in the narrow regions close to the spacers and far outside the nanoimprint field, so that a uniform contact within the nanoimprint field is achieved. For the same reason, the relative lateral shifts between the mask and the substrate is <2.4 nm within the field (Figure 4); in short, these simulations confirmed our expectations that the lateral shift in the quality area will be small. Fundamentally, this is because the lateral length of the bowing region is about 10^4 times the vertical movement. More importantly, the small shift is predictable and can be compansated by DFM (Designed-For-Manufacturing) software.

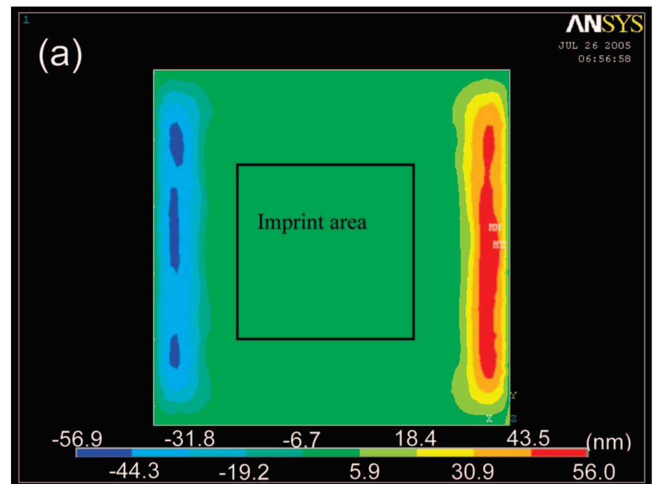

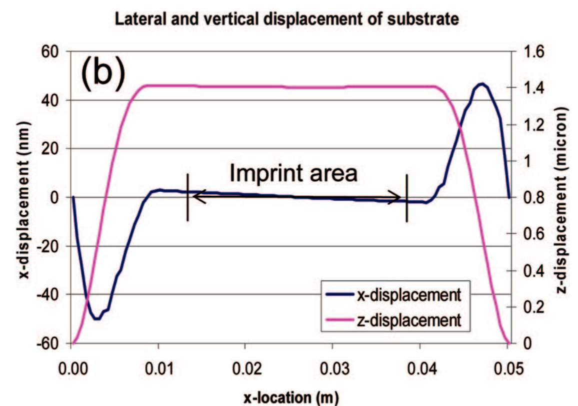

Figure 4. Numerical simulation (FEM) results of the wafer lateral displacement as a result of the wafer bowing. (a) The 2D map of the wafer displacement in the "*x*" direction. (b) The profile of both "*x*" (blue dots) and "*z*" (purple dots) displacements of the wafer as a result of the wafer bowing. The lateral displacement within the imprint field is less than 2.4 nm.

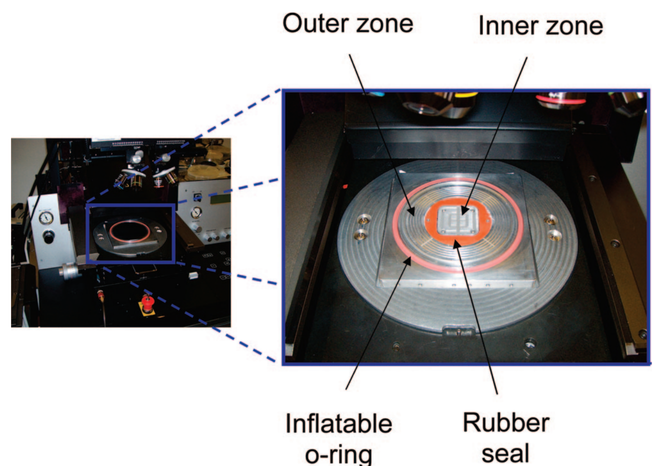

Figure 5. A contact mask aligner with a nanoimprint module loaded. The mask aligner is transformed into a nanoimprint machine.

Experimental Results. We designed and constructed a nanoimprint module that can be incorporated into a mask aligner (Figure 5), which is thus transformed into a nanoimprinter capable of performing the entire nanoimprint process including alignment, nanoimprint, and mold/sample separa-

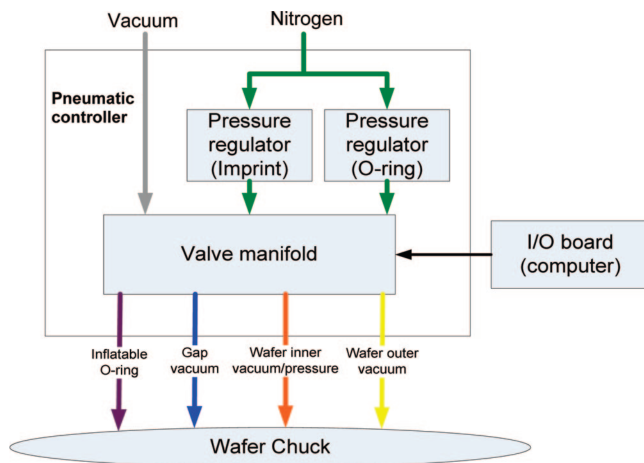

Figure 6. Schematic diagram of the nanoimprint module.

tion. Figure 6 shows the schematic diagram of the module. There are two main parts: a wafer chuck and a pneumatic controller. The wafer chuck replaces the wafer chuck on the mask aligner and performs the wafer bowing nanoimprint. The wafer chuck is divided into two zones: an outer zone and an inner zone, which are separated by a rubber seal (Figure 5). The outer zone of the chuck works as a normal vacuum chuck to hold the wafer, and the inner zone is switchable between vacuum and pressure. An inflatable O-ring slightly larger than the wafer is located at the rim of the wafer chuck. When inflated, it touches the mask and a sealed chamber is formed between the mask and the wafer. Venting/pumping holes on the chuck close to the inner edge of the O-ring are used to apply vacuum or pressure in the gap between the wafer and the mask. The entire nanoimprint process (Figure 1) is realized through a sequence of pumping/venting of the inner chuck zone, gap vacuum/venting and O-ring inflation/deflation. The sequence is controlled by a computer-driven pneumatic controller. On the inlet side, the pneumatic controller connects to a vacuum supply and a pressurized N_2 source; on the outlet side, it supplies four pneumatic lines to the wafer chuck. Those lines connect to the inflatable O-ring, the gap between the wafer and the mask, the wafer chuck inner zone and the outer zone respectively. The pressures of the inflatable O-ring and the wafer inner zone are adjustable via two pressure regulators (SMC AR20-NO1-Z). Those pneumatic outputs are controlled by a set of electric valves (SMC VQC1100NR-5), which are controlled by purpose-written software through a digital I/O board (NI 6514).

The process we implemented in the module was a UV-curable nanoimprint with a double layer of spin-coated resists.[3] During the nanoimprint process, a mask (mold) with spacers was loaded onto the mask holder in the same way as a photomask, and a wafer with a spin-coated transfer layer and imaging layer was loaded onto the nanoimprint chuck. A vacuum was then applied to both the inner and the outer zones on the imprint module. The coarse alignment procedure was exactly the same as photolithography alignment. The spacers on the mask are brought into contact with the wafer by using the "alignment check" function of the mask aligner (SUSS MicroTec MA-6), and fine alignment was performed. After that, the O-ring was inflated, the gap between the mold and wafer was evacuated, and the inner zone was pressurized. The center of the wafer was pushed toward the mask under the differential pressure and the resist was imprinted by the mold. The approach and imprint step was completed by using the "exposure" functionality of the mask aligner to cure the imaging layer of the resist. Finally, the inner zone was evacuated, the gap was vented to air, and the O-ring was deflated. The mask and the wafer were released by the vacuum at the back of the wafer. Both the imprinted wafer and the mold were unloaded from the mask aligner in the same fashion as unloading an exposed wafer and photomask in photolithography.

In our experimental setup, the mold is fabricated on a standard 5 in. quartz mask blank either by e-beam lithography (EBL) directly or by NIL using a Si mold made by EBL,[6] with a field size of 25.4 mm $\times$ 25.4 mm. Although the module is capable of a high imprint pressure, a gas pressure of only about 1 atm. is normally used. The feature size

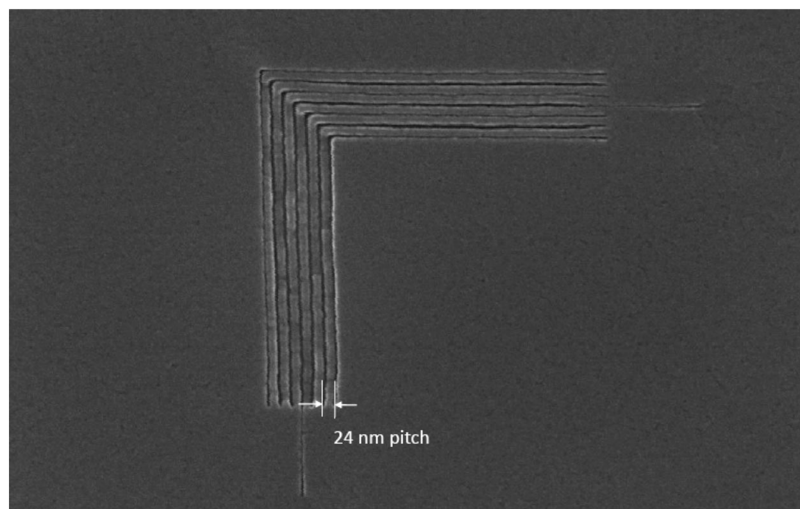

Figure 7. SEM image of nested Ls in nanoimprint resist at 12 nm half-pitch fabricated using the nanoimprint process based on wafer bowing.

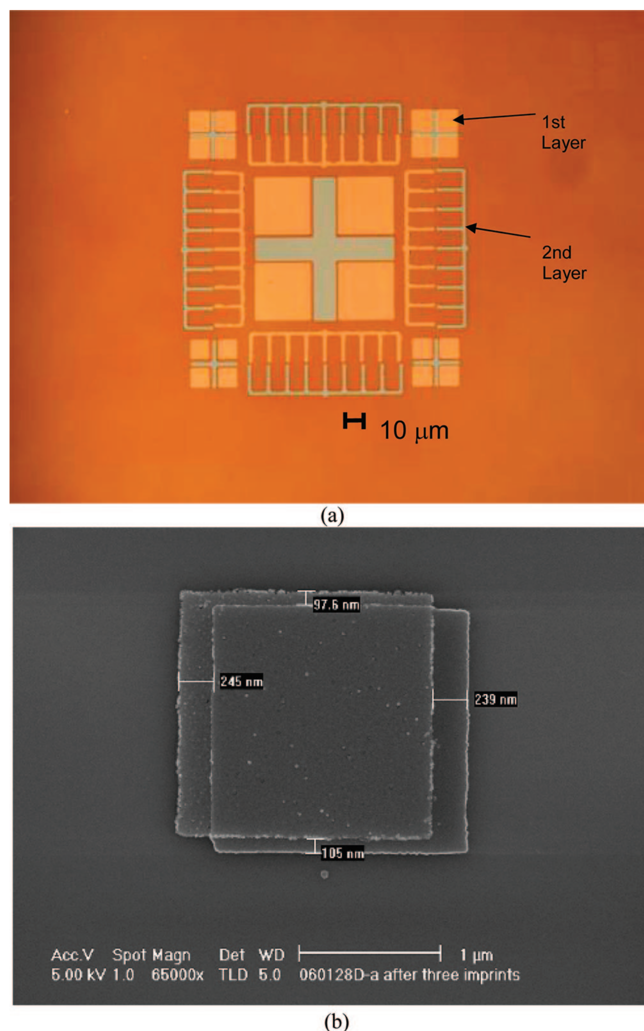

Figure 8. (a) Optical image of the alignment marks from two sequential nanoimprints, showing that the alignment accuracy is better than a half-micron (optical resolution). (b) SEM image of two square shape patterns fabricated by two sequential nanoimprint steps. A misalignment of about a quarter micron is shown in the image.

resolution of this nanoimprint module is <10 nm, illustrated by Figure 7, which shows a scanning electron microscope (SEM) image of nested Ls at 12 nm half-pitch in imprinted nanoimprint resist. Both dense lines at 12 nm half-pitch, isolated line with line-width less than 10 nm and sharp corners were successfully imprinted.

Figure 8a,b shows the alignment results of better than 0.5 μm of overlay. Figure 8a is an optical image of the alignment markers. The yellowish marker was defined in the first layer nanoimprint and the bluish one was defined in the second layer. The image shows no obvious misalignment within the optical microscope resolution. On the basis of the SEM image (Figure 8b) of two square patterns designed to be overlapping, the misalignment was better than 0.5 μm. The alignment accuracy of better than 0.5 μm, which was the resolution limit of our microscope, was maintained over the whole imprint field. The overlay performance of this imprint module is limited by the resolutions of the microscope and of the Vernier patterns, not by the wafer-bowing technology.

Summary. We introduced the concept of wafer bowing to affect nanoimprinting and developed the nanoimprint process based on wafer bowing. This approach enables the key imprinting mechanism to be designed into a compact module. We have constructed such a module and demonstrated an overlay and resolution of <0.5 μm and <10 nm, respectively. In the short term, this approach makes high-quality nanoimprint lithography much more accessible to a broad range of researchers. More importantly, this approach minimizes local mechanical movement and greatly shortens the mechanical path between the mold and the wafer; this will enable achieving excellent overlay at a low cost. In the long term, our method is extensible to step-and-repeat printing for volume manufacturing.

Acknowledgment. K.K.B. thanks King Abdulaziz City for Science and Technology and Alfaisal University for partially supporting EBL writing of the mold.

References

(1) Chou, S. Y.; Krauss, P. R.; Renstrom, P. J. *J. Vac. Sci. Technol., B* **1996**, *14*, 4129.
(2) Jung, G.-Y.; Johnston-Halperin, E.; Wu, W.; Yu, Z.; Wang, S.-Y.; Tong, W. M.; Li, Z.; Green, J. E.; Sheriff, B. A.; Boukai, A.; Bunimovich, Y.; Heath, J. R.; Williams, R. S. *Nano Lett.* **2006**, *6*, 351.
(3) Wu, W.; Jung, G. Y.; Olynick, D. L.; Straznicky, J.; Li, Z.; Li, X.; Ohlberg, D.; Chen, Y; Wang, S. Y.; Tong, W. M.; Williams, R. S. *Appl. Phys. A: Mater. Sci. Process* **2005**, *80*, 1173.
(4) Wu, W.; Kim, E.; Ponizovskaya, E.; Liu, Y.; Yu, Z.; Fang, N.; Shen, Y. R.; Bratkovsky, A. M.; Tong, W.; Sun, C.; Zhang, X.; Wang, S. Y.; Williams, R. S. *Appl. Phys. A: Mater. Sci. Process.* **2007**, *87*, 143.
(5) Kim, E.; Wu, W.; Ponizovskaya, E.; Yu, Z.; Bratkovsky, A. M.; Wang, S.-Y.; Williams, R. S.; Shen, Y. R. *Appl. Phys. Lett.* **2007**, *91*, 3105.
(6) Yang, J. K. W.; Berggren, K. K. *J. Vac. Sci. Technol., B* **2007**, *25*, 2025.

NL802295N